Atmos. Meas. Tech. Discuss., 8, 8191–8230, 2015
www.atmos-meas-tech-discuss.net/8/8191/2015/
doi:10.5194/amtd-8-8191-2015

Atmospheric Measurement Techniques Discussions

Retrieval algorithm for rainfall mapping from microwave links in a cellular communication network

A. Overeem[1,2], **H. Leijnse**[2], **and R. Uijlenhoet**[1]

[1]Hydrology and Quantitative Water Management Group, Wageningen University, P.O. Box 47, 6700 AA, Wageningen, the Netherlands
[2]Royal Netherlands Meteorological Institute (KNMI), P.O. Box 201, 3730 AE, De Bilt, the Netherlands

Received: 18 July 2015 – Accepted: 20 July 2015 – Published: 7 August 2015

Correspondence to: A. Overeem (overeem@knmi.nl)

Published by Copernicus Publications on behalf of the European Geosciences Union.

Abstract

Microwave links in commercial cellular communication networks hold a promise for areal rainfall monitoring and could complement rainfall estimates from ground-based weather radars, rain gauges, and satellites. It has been shown that country-wide rainfall maps can be derived from the signal attenuations of microwave links in such a network. Here we give a detailed description of the employed rainfall retrieval algorithm and provide the corresponding code. Moreover, the code (in the scripting language "R") is made available including a data set of commercial microwave links. The purpose of this paper is to promote rainfall monitoring utilizing microwave links from cellular communication networks as an alternative or complementary means for global, continental-scale rainfall monitoring.

1 Introduction

Accurate rainfall observations with high spatial and temporal resolution are needed for hydrological applications, agriculture, meteorology and weather forecasting, and climate monitoring. However, there is a lack of accurate rainfall information for the majority of the land surface of the earth, notably from ground-based weather radars (Heistermann et al., 2013). Moreover, the number of reporting rain gauges is dramatically declining in Europe, South America, and Africa (a decline of approximately 50 % in the period 1989–2006 for GPCC, version 5.0 according to Lorenz and Kunstmann (2012). Satellites are often the only source of rainfall information. Despite their increasing coverage and spatio-temporal resolution, measurement errors and sampling uncertainties limit the stand-alone applicability of satellite rainfall products. This calls for alternative and complementary sources of rainfall information. Since 2006 various studies have shown that microwave links from operational cellular communication networks may be used for rainfall monitoring (e.g., Messer et al., 2006; Leijnse et al., 2007a; Zinevich et al., 2009; Overeem et al., 2011, 2013; Chwala et al., 2012; Rayitsfeld et al., 2012;

AMTD
8, 8191–8230, 2015

Bianchi et al., 2013; Doumounia et al., 2014). The ability to observe other types of precipitation, such as snow, is limited.

The basic principle of rainfall estimation using microwave links is as follows. Rainfall attenuates the electromagnetic signals transmitted from the circular antenna of one telephone tower to another (Fig. 1). By taking the measured received power at one end of a microwave link as a function of time (stored operationally by communication companies to monitor the quality of their networks), the rainfall-induced path-integrated attenuation can be calculated, which can be converted to average rainfall intensities over the path of a link. This is particularly interesting for those countries where few surface rainfall observations are available.

Based on a 12 day data set Overeem et al. (2013) have shown that country-wide ($\approx 35\,000\,km^2$) rainfall maps can be derived from received signal powers of microwave links in a cellular communication network. Rainfall estimation employing the cellular communication network was shown to work successfully for a relatively large data set in space and time. Hence, further upscaling this novel source of rainfall information is the logical next step toward global, continental-scale rainfall monitoring. The underlying rainfall retrieval algorithm is briefly described in Overeem et al. (2013), and largely based on Overeem et al. (2011). The purpose of this paper is to provide a detailed description of a slightly modified version of the algorithm of Overeem et al. (2013) and the corresponding computer code, as well as to provide open access to the code. A working example (see Supplement) is provided to compute link-based rainfall maps for the entire surface area of the Netherlands for one day from real microwave link data as used in Overeem et al. (2013). Note that link data are utilised in a stand-alone fashion to obtain rainfall information, i.e., data from rain gauges, weather radars, or satellites are not combined with the link data.

This paper is organised as follows. First a description of the required microwave link data is given. Next, the rainfall retrieval algorithm and the interpolation methodology are described, accompanied by examples. Attention is given to the main retrieval issues associated with link-based rainfall estimation: decrease in signal levels during non-rainy

AMTD
8, 8191–8230, 2015

periods, wet antenna attenuation, and temporal sampling strategy. Finally, conclusions and a discussion are given.

2 Data

2.1 Microwave link data: characteristics and preparations

2.1.1 Employed data sets

In order to compute path-averaged rainfall intensities, received signal powers were obtained from microwave links in a cellular communication network in the Netherlands, operated by T-Mobile NL. The minimum and maximum received powers over 15 min intervals were provided, based on 10 Hz sampling. The transmit power may be assumed constant. The data have a resolution of 1 dB, and the majority of these Nokia links use vertically polarised signals. Signal powers are commonly stored at 0.1 or even at 1 dB resolution. This may lead to quantisation errors. Many links are full-duplex, i.e., those links measure in two directions over the same link path.

The accuracy of the link coordinates has been rounded (≈ 100 m) due to confidentiality requirements from the cellular communication company involved. It is advised to use a higher accuracy in applications of the retrieval algorithm and computer code elsewhere. The majority of the provided links does not exist anymore due to network renewal and deployment of underground fiber optical cable networks. Data were obtained from 9 September, 08:00 UTC–11 September, 08:00 UTC (2011), to estimate rain for 10 September, 08:00 UTC–11 September, 08:00 UTC. Figure 1 shows the locations of links used to estimate rainfall for this day (on average 2309 links and 1440 link paths over all 96 time intervals of 15 min). Note the gap in the link network, which is also reported by Rios Gaona et al. (2015) for a 12 day data set including the day used here. This is mainly caused by data storage issues with the cellular communication company. Hence, this is not related to the malfunctioning of microwave links as such.

AMTD
8, 8191–8230, 2015

Also data from two other days are used to illustrate the rainfall retrieval algorithm, but these data are not released with this paper. All link data are from a validation data set, i.e., they have not been used to calibrate the rainfall retrieval algorithm.

2.1.2 Data format used in code

The code is designed for estimating rainfall from minimum and maximum received powers over time intervals of a given length. Data are processed on a daily basis. For each link and time interval the following variables are needed in ASCII file format: microwave frequency f (GHz), date and end time of observation (YYYYMMDDhhmm, i.e., year (2011), month (09), day (11), hour (08), minutes (00): 201109110800), minimum and maximum received power P_{min} and P_{max} (dBm), path length L (km), coordinates (longitude and latitude) of start and end of link in WGS84 (degrees), and unique link identifier (ID), which should remain the same over all days. A full-duplex link should have two IDs, one for each link direction. Note that a header should be provided as given in the data files from the example. Table 1 gives an overview of the variables, including header names for all programs in the rainfall retrieval algorithm. The order of the columns does not matter, as long as the variable name matches the column. IDs are handled as strings. Hence, not only integers, but, for instance, also alphanumeric ID's can be used.

A constant transmit power is assumed. This will be a reasonable assumption for many networks (Messer et al., 2006; Leijnse et al., 2007a; Chwala et al., 2012; Rayitsfeld et al., 2012; Bianchi et al., 2013). For other networks the transmit power is allowed to fluctuate in order to compensate for large losses along the link path. This is the case when Automatic Transmit Power Control (ATPC) is activated. The code will also work for other periods than 08:00 UTC previous day–08:00 UTC present day, as long as the same daily period is used for each file, in correspondence with the chosen period in the program "Preprocessing_Linkdata.R". The programs explicitly employs the UTC time zone. This can be easily changed into another time zone, but this can lead to problems in case of transition to and from daylight saving time. Hence, it is recommended to use

AMTD
8, 8191–8230, 2015

a time zone without daylight saving, such as UTC. Note that missing link data are allowed, i.e., the code will work if a time interval has no data. Though many missing data may lead to rainfall intensities not being calculated.

2.2 Gauge-adjusted radar rainfall depths

Overeem et al. (2013) use a gauge-adjusted radar data set with a spatial resolution of approximately 0.9 km^2 to calibrate the microwave link rainfall retrieval algorithm. Here this radar data set is utilised to validate link-based rainfall maps. More information on the derivation of this data set can be found in Overeem et al. (2009a, b, 2011).

3 Methodology

This section describes the entire processing chain from received signal powers to rainfall maps. The link data have to be supplied in the format described above. Figure 2 gives the processing flowchart. The code is provided as R scripts, which are run in the free software environment R (http://www.r-project.org/), which is available for Linux, OS X, and Windows operating systems. The following R packages need to be installed: "ggmap", "ggplot2", "grid", "gstat", "labeling", "maps", "mapproj", "rgdal", and "sp".

3.1 Preprocessing of link data

The flowchart starts with the preprocessing of link data using the program "Preprocessing_Linkdata.R", which does the following:

1. Data from previous and present 24 h period are read. If one or both files are not available, processing stops.

2. Time interval numbers are computed from the provided date and time. The first time interval of the previous 24 h period gets number 1, the second time interval

AMTD
8, 8191–8230, 2015

gets number 2, et cetera. The number of the last time interval of the present 24 h period is the total number of time intervals in 48 h.

3. It is important that the value of the exponent *b* in Fig. 5 (right) is close to 1, which is the case for a range of frequencies. Here, only links with microwave frequency from 12.5–40.5 GHz are selected. The chosen frequencies can be altered in the script.

4. For each unique link identifier a time interval is removed if it contains more than one record.

5. If no link data are available anymore for the selected unique link identifier for the present 24 h period, perform the previous step for the next unique link identifier.

6. For each unique link identifier it is checked whether its frequency, link coordinates, or path length vary during the day. If this is the case for one of these variables, the link is discarded for this particular day.

7. The link coordinates in WGS84 (degrees) are converted to an Azimuthal Equidistant Cartesian coordinate system (easting and northing of start of link, easting and northing of end of link, respectively; km). The middle of this coordinate system has to be provided in the script as longitude and latitude in WGS84 coordinates (degrees).

8. The link data are written to a file. Data from previous and present 24 h period are combined into one file for each day for which rainfall maps need to be obtained. Data from the previous 24 h period are needed for a reliable wet-dry classification and determination of the reference signal level. The format of the output file is the same as the format of the input file, except that it contains an additional column with the time interval number.

9. Repeat these steps for each unique link identifier in the present 24 h period.

AMTD
8, 8191–8230, 2015

In the working example, time interval number 1 runs from 08:00–08:15 UTC of previous day, time interval number 2 runs from 08:15–08:30 UTC of previous day, et cetera. The last time interval covers 07:45–08:00 UTC of present day. Link data from the previous 24 h period are only used if the corresponding link also has any link data for the present 24 h period. The selections above reduce the number of links from 2612 to 2472.

3.2 Classification of wet and dry periods: the link approach

The received signal powers often decrease during non-rainy periods, resulting in non-zero rainfall estimates, e.g., caused by reflection of the beam or dew formation on the antennas (see Upton et al., 2005, for an overview). To prevent this rainfall overestimation a reliable classification of wet and dry periods is needed. This is also beneficial for determining an appropriate reference signal level, representative for dry weather. Different classification methods have been proposed, of which some can be applied to received powers or signal attenuations when they are sampled at very high frequency, e.g., every 6 or 30 s (Schleiss and Berne, 2010), or even at 20 GHz. For instance, Chwala et al. (2012) present a spectral time series analysis, and Wang et al. (2012) Markov switching models. Here the so called "link approach" is employed (Overeem et al., 2011, 2013), which was derived for application to minimum received powers over a time interval (15 min in Overeem et al., 2011, 2013). A common sampling strategy for commercial microwave links is to obtain a minimum and maximum power per 15 min interval (Messer et al., 2006; Overeem et al., 2011, 2013). Sometimes powers are sampled every second (Doumounia et al., 2014), every minute (Rayitsfeld et al., 2012), or only once or twice every 15 min (Leijnse et al., 2007a). Other approaches to identify rainy and non-rainy spells make use of auxiliary sources, but are not considered in this paper. For instance, radar data have been utilised in "the radar approach" (Overeem et al., 2011), and satellite data in the "satellite approach" (Van het Schip et al., 2015).

Starting point are the minimum and maximum received powers over a given time interval (15 min in this case), as shown in Fig. 3a for one link during 24 h. This exam-

AMTD
8, 8191–8230, 2015

ple is meant as a successful illustration of the rainfall retrieval algorithm. As expected, there is a strong negative correlation between the minimum received powers and the path-averaged gauge-adjusted radar rainfall intensities. In order to define wet and dry periods, we assume that rain is correlated in space, and hence that several links in a given area should experience a decrease in received signal level in the case of rain. A time interval is labeled as wet if at least half of the links in the vicinity (radius of 15 km) of the selected link experience such a decrease. The program "WetDryClassification_LinkApproach.R" performs the wet-dry classification according to this link approach. A step-by-step description of the classification algorithm is given below and mainly obtained from Overeem et al. (2011):

1. In a given 24 h period, select a link.
2. All links for which both end points are within 15 km from either end of the already selected link are selected as well.
3. Continue if at least 3 surrounding links have been selected for all time intervals of previous and present 24 h period for which the link in step 1 has data, otherwise the link is not used. In that case go to step 1 and select another link. If the link is part of a full-duplex link, the other link is counted as surrounding link.
4. Calculate the attenuation $\Delta P = P_{\mathrm{min}} - \max(P_{\mathrm{min}})$ and specific attenuation $\Delta P_{\mathrm{L}} = \frac{P_{\mathrm{min}} - \max(P_{\mathrm{min}})}{L}$ for each link and each time interval. $\max(P_{\mathrm{min}})$ is the maximum value of P_{min} over the previous 24 h before the present time interval. For the previous 24 h period, the maximum value over this entire period is used. Note that $\max(P_{\mathrm{min}})$ is only computed in case of at least 6 h of data, otherwise it is not available and no rainfall intensities will be computed.
5. The median values of ΔP and ΔP_{L} are computed over all selected links for each time interval.
6. If $\mathrm{median}(\Delta P_{\mathrm{L}}) < -0.7\,\mathrm{dB\,km^{-1}}$ and $\mathrm{median}(\Delta P) < -1.4\,\mathrm{dB}$ the time interval is classified as wet for the link selected in step 1.

AMTD
8, 8191–8230, 2015

7. If $\max(P_{\min}) - P_{\min} > 2$ dB for a given time interval that is classified as wet, the previous two time intervals and the next time interval are classified as wet for the link selected in step 1.

8. All time intervals that have not been classified as wet are classified as dry for the link selected in step 1.

9. Repeat these steps for all other links and every available 24 h period.

The threshold values in steps 6 and 7 have been obtained from Overeem et al. (2011), who optimise them by visual comparison with the gauge-adjusted radar data set of path-averaged rainfall intensities employing data from 2009 (NEC links with 0.1 dB power resolution). Note that a radius of 10 km is used in Overeem et al. (2011), whereas a radius of 15 km is used here and in Overeem et al. (2013), which allows estimating rainfall in areas with lower link density. The 15 km radius is of the order of the decorrelation distance of rainfall in the Netherlands (Overeem et al., 2011). Step 3 has been slightly altered with respect to Overeem et al. (2011).

3.3 Determination of reference signal level and of corrected received powers

Now the rainy and non-rainy time intervals have been classified, an accurate reference signal level or base level, representative of dry weather, is computed. Moreover, corrected received minimum and maximum powers are calculated. The reference signal level P_{ref} is computed for each link and time interval separately as follows:

1. Compute $\overline{P} = \frac{P_{\min}+P_{\max}}{2}$ (in dBm), for each time interval classified as dry in the previous 24 h before the present time interval.

2. P_{ref} is the median of $\overline{P}$ over all those time intervals if the number of dry time intervals represents at least 2.5 h in the previous 24 h, or 10.4 %. Otherwise P_{ref}, and hence the rainfall intensity, are not available, so not computed.

AMTD
8, 8191–8230, 2015

Subsequently, corrected minimum (P^{C}_{min}) and maximum (P^{C}_{max}) received powers are computed:

$$P^{C}_{min} = \begin{cases} P_{min} & \text{if} \quad \text{wet AND } P_{min} < P_{ref}, \\ P_{ref} & \text{if} \quad \text{dry OR } P_{min} \geq P_{ref}. \end{cases} \tag{1}$$

$$P^{C}_{max} = \begin{cases} P_{max} & \text{if} \quad P^{C}_{min} < P_{ref} \text{ AND } P_{max} < P_{ref}, \\ P_{ref} & \text{if} \quad P^{C}_{min} = P_{ref} \text{ OR } P_{max} \geq P_{ref}. \end{cases} \tag{2}$$

Fig. 3 shows the corrected received powers and the reference level (b). In this particular example hardly any corrections are made. Figure 4 shows another example, meant to illustrate the necessity of a wet-dry classification. No rain is observed by weather radars combined with rain gauges, whereas minimum received powers severely decline (a). The link approach successfully corrects for this, as can be seen by the corrected received powers becoming equal to the reference level (b). The program "WetDryClassification_LinkApproach.R" is used to determine P_{ref}, P^{C}_{min}, and P^{C}_{max}.

3.4 Filter to remove outliers

Malfunctioning link antennas can cause outliers in rainfall retrievals (especially for daily accumulations). These outliers can be removed by using a filter that is based on the assumption that rainfall is correlated in space. The filter discards a time interval of a link for which the cumulative difference between its specific attenuation and that of the surrounding links over the previous 24 h (including the present time interval) becomes lower than $-32.5\,\mathrm{dB\,km^{-1}}$ h. This criterion is applied to specific attenuation

AMTD
8, 8191–8230, 2015

derived from minimum received power (Overeem et al., 2013). The value of the filter F is computed as follows:

$$F = \sum_{t=-24+\Delta t\,\mathrm{h}}^{0} \left(\Delta P_{\mathrm{L},t}^{\mathrm{S}} - \mathrm{median}(\Delta P_{\mathrm{L},t})\right) \Delta t, \quad (3)$$

where t is the time interval, $t = 0$ being the present time interval for which F needs to be computed, and Δt is the time interval in hours (0.25 h in the working example). Note that $t = -23.75$ h holds for a 15 min time interval. The general expression is $t = -24$ h minus the time interval (h). A link is not used to estimate rainfall if $F < -32.5\,\mathrm{dB\,km^{-1}}$ h, corresponding to $-130\,\mathrm{dB\,km^{-1}}$ over the considered 24 h period. Note that $\Delta P_{\mathrm{L}}^{\mathrm{S}}$ and median(ΔP_{L}) are computed in the link approach and are based on the minimum received powers, the superscript S referring to the selected link for which rainfall is to be computed. The program "WetDryClassification_LinkApproach.R" computes the value of F, but the application of the filter is performed by the program "RainfallRetrieval_Links.R". The maximum rainfall amount which would not be filtered out cannot be exactly computed, for instance, because F is not based on the maximum received power and because ΔP_{L} has been computed with respect to the maximum value of the minimum received power and not the reference signal level. Nevertheless, the following example gives an indication. Imagine that the $32.5\,\mathrm{dB\,km^{-1}}$ h is constantly distributed over all time intervals in a 24 h period. This implies a maximum specific attenuation of approximately $1.35\,\mathrm{dB\,km^{-1}}$ ($32.5\,\mathrm{dB\,km^{-1}}$ h divided by 24 h) per time interval. Next, the path-averaged maximum rainfall intensity is computed using Eq. (4) (see next subsection). It is around $5\,\mathrm{mm\,h^{-1}}$ for $f = 38.9$ GHz (a representative microwave frequency), implying this would need to occur during all time intervals from a 24 h period. Hence, a time interval of a chosen link will only be discarded if the rainfall amounts during the previous 24 h period are substantial (i.e., 120 mm). Moreover, here it is assumed that the other links do not have rain-induced attenuation. Surrounding links are likely affected in case of large rainfall amounts. In that case even larger attenuations would be

AMTD
8, 8191–8230, 2015

required for the link under consideration to be discarded. It is therefore highly unlikely that this filter would discard real rain. The filter to remove outliers leads to a further reduction from 2428 to 2399 links for the working example.

3.5 Computation of path-averaged rainfall intensities

3.5.1 Basic principle

Rainfall intensity can be estimated from microwave specific attenuation k ($\mathrm{dB\,km^{-1}}$) using a power law R–k relation (Atlas and Ulbrich, 1977; Olsen et al., 1978):

$$R = a\,k^{b}, \tag{4}$$

where R is the rainfall intensity ($\mathrm{mm\,h^{-1}}$). Coefficients a ($\mathrm{mm\,h^{-1}\,dB^{-b}\,km^{b}}$) and exponents b (–) depend mainly on link frequency. The values of a and b used in this study are derived from measured drop size distributions (Leijnse et al., 2008), and are shown as functions of link frequency in Fig. 5. The relative decrease in microwave link signal power is related to the attenuation A_m (dB) over the link with length L (km), and thus to the rainfall intensity:

$$P_\mathrm{ref}(L) - P(L) = A_\mathrm{m} = \int_0^L k(s)\mathrm{d}s = \int_0^L \left(\frac{R(s)}{a}\right)^{1/b} \mathrm{d}s, \tag{5}$$

where P is the received signal power (dBm), P_ref the base line or reference signal level, and s the distance along the link (km). Because of the nonlinearity of the integrand of Eq. (5), we need to make assumptions about the distribution of $R(s)$ in order to derive a relation between $P(L)$ and the path-averaged rainfall intensity. Here we assume

AMTD
8, 8191–8230, 2015

that the point-scale R–k relation provides a good approximation for the path-averaged rainfall intensity $\langle R \rangle$ (mm h^{-1}) as well:

$$A_{\mathrm{m}} = L\langle k \rangle \approx L\left(\frac{\langle R \rangle}{a}\right)^{1/b}, \tag{6}$$

where $\langle k \rangle$ is the path-averaged (specific) attenuation (dB km^{-1}). The path-averaged rainfall intensity $\langle R \rangle$ can now be expressed as:

$$\langle R \rangle = a\left(\frac{P_{\mathrm{ref}}(L) - P(L)}{L}\right)^{b}. \tag{7}$$

For the link frequencies employed in this study (between 13 and 40 GHz) the value of the exponent b is close to 1 (Fig. 5, right). Because of this near-linearity of the integrand in Eq. (5), the assumption on the distribution is not very strong, leading to limited errors caused by using the approximation in Eq. (6). This was also shown by Berne and Uijlenhoet (2007); Leijnse et al. (2008, 2010); Overeem et al. (2011).

3.5.2 Computation of mean path-averaged rainfall intensities

Here the path-averaged rainfall intensities are computed from the corrected minimum and maximum received signal powers. The minimum and maximum rain-induced attenuation are calculated for each link and time interval using:

$$\begin{aligned} A_{\mathrm{min}} &= P_{\mathrm{ref}} - P^{\mathrm{C}}_{\mathrm{max}}, \\ A_{\mathrm{max}} &= P_{\mathrm{ref}} - P^{\mathrm{C}}_{\mathrm{min}}. \end{aligned} \tag{8}$$

AMTD
8, 8191–8230, 2015

Next, the minimum and maximum path-averaged rainfall intensities are computed:

$$\langle R_{\min} \rangle = a \left(\frac{A_{\min} - A_a}{L} H(A_{\min} - A_a) \right)^b, \quad (9)$$

$$\langle R_{\max} \rangle = a \left(\frac{A_{\max} - A_a}{L} H(A_{\max} - A_a) \right)^b, \quad (10)$$

with H the Heaviside function (if the argument of H is smaller than zero, $H = 0$; else $H = 1$). Attenuation due to wet antennas gives rise to overestimation of rainfall and needs to be compensated for (Kharadly and Ross, 2001; Minda and Nakamura, 2005; Leijnse et al., 2007a, b, 2008). Hence, A_a is introduced, meant for correcting attenuation due to wet antennas (dB), and assumed to be constant, e.g., independent of rain rate and frequency. The coefficients a and b are valid for vertically polarised signals (Fig. 5), which will usually be employed for microwave links. They may also be applied to links with horizontally polarised signals, since the values for a (at least for f around 13–39 GHz) and for b (at least for f around 38–39 GHz) are almost the same as those for horizontally polarised signals. The values of b deviate somewhat more for f between 15–35 GHz. To conclude, the utilised coefficients will give some errors in the retrieved rainfall estimates for horizontally polarised signals.

Note that the program "WetDryClassification_LinkApproach.R" computes $A_{\min}$, $A_{\max}$, and gives the values for a and b. The output of this program is: link identifier, a (mm h^{-1} dB^{-b} km^b), b (–), $A_{\max}$ (dB), $A_{\min}$ (dB), L (km), time interval number (only present 24 h period), coordinates of link (km), the average number of surrounding links including the selected one over the time intervals for which the selected link is available ("meanval"; full-duplex links are counted twice), F (dB km^{-1} h), f (GHz), $P_{\min}$ (dB), $P_{\max}$ (dB), $P^{C}_{\min}$ (dB), $P^{C}_{\max}$ (dB), P_{ref} (dB), date and time (YYYYMMDDhhmm). The actual application of the rainfall retrieval algorithm is done by the program "RainfallRetrieval_Links.R".

AMTD
8, 8191–8230, 2015

The assumed temporal sampling strategy only provides a minimum and maximum power over a given time interval. The mean path-averaged rainfall intensity is computed as follows:

$$\langle R \rangle = \alpha \langle R_{\max} \rangle + (1 - \alpha) \langle R_{\min} \rangle, \quad (11)$$

where α is a coefficient that determines the contribution of the minimum ($R_{\min}$) and maximum ($R_{\max}$) path-averaged rainfall intensity (mm h^{-1}) during a time interval. Overeem et al. (2011) optimise A_a and α for two frequency classes, whereas this has been reduced to one frequency class for Overeem et al. (2013). The values for A_a (2.3 dB) and α (0.33) have been taken from Overeem et al. (2013), who use a 12 day calibration data set from June and July 2011. They compare daily link-based rainfall depths with gauge-adjusted radar retrievals to calibrate the rainfall retrieval algorithm. Note that the value of α presented here is based on data available at 15 min time intervals. It is expected that this value will be different for disparate time intervals.

Figure 3 shows the minimum and maximum path-averaged link rainfall intensities (c), the mean path-averaged link and gauge-adjusted rainfall intensities (d), the cumulative link and gauge-adjusted rainfall depths (e), as well as the location of the microwave link in the middle of Amsterdam, the Netherlands (f). The mean path-averaged link rainfall intensities and the cumulative link rainfall depths correspond well with the gauge-adjusted radar-based values. Figure 4 shows these results for another link on a dry day when no link approach would have been applied. The graph of cumulative rainfall depth (e) shows an overestimation of 7 mm for the link in Spijkenisse, the Netherlands (f). This illustrates that the link approach is indispensable. Figure 6 is based on data from the working example and also illustrates the different steps in the rainfall retrieval algorithm. It shows the results for one link close to the city centre of Utrecht, and is meant to depict deviations in link-based rainfall retrievals. This figure can be obtained by running R script "Figure_Timeseries_Power_Rainfall.R", which is possible if "WetDryClassification_LinkApproach.R" has been run. The program also reads a file

AMTD
8, 8191–8230, 2015

with path-averaged gauge-adjusted 15 min radar rainfall depths. The dynamics of the rainfall event are similar for links and radars combined with rain gauges, but the link observes much more rainfall, 88 % more for the total accumulation. These differences are hard to explain, although the following factors likely make a large contribution. Representativeness errors may play a large role given the local convective character of this rainfall event (also see the rainfall maps described in the next subsection). Perhaps attenuation due to wet antennas is relatively large due to a thick water layer caused by intense rainfall, leading to an overestimation of link rainfall depths. In addition, the radar rainfall data have been obtained from a composite based on data from two radars. For the selected link path in Utrecht, which is close to the radar in De Bilt (lower white circle in Fig. 1), the composite is primarily based on the data from the radar in Den Helder (upper white circle in Fig. 1), at approximately 100 km distance. Attenuation along the radar beam, as well as radome attenuation may have resulted in a strong decrease in the radar rainfall estimates.

The program "RainfallRetrieval_Links.R" gives the following output: link identifier, mean path-averaged link rainfall depth (mm), L (km), coordinates of link (km), time interval number (only present 24 h period), and f (GHz).

3.6 Rainfall maps

Here ordinary kriging is used to obtain rainfall maps. Kriging is well-suited for dealing with heterogeneously distributed data locations. This method requires a variogram model, but unfortunately it is impossible to robustly estimate such variograms for each time interval separately due to the sparsity of rainfall. Hence, a more robust procedure is followed. The sill and range of an isotropic spherical variogram model have been expressed as a function of day of year (DOY) and duration (1–24 h) using rain gauge data from the Netherlands (Van de Beek et al., 2012). If needed the relationships can be extrapolated to time intervals shorter than 1 h. The nugget is set equal to 0.1 times the sill. Note that these equations and the optimal values of their coefficients have been found to be useful for the Dutch climate.

AMTD
8, 8191–8230, 2015

Interpolated rainfall maps are provided by program "Interpolation_Rainfall_Intensities.R". It performs the following steps:

1. Read the interpolation grid with coordinates (longitude and latitude) in WGS84 (two columns, degrees). In this case a radar grid is used, where each grid cell represents the middle of the radar pixel. The coordinates are converted to an Azimuthal Equidistant Cartesian coordinate system (easting and northing; km). The middle of this coordinate system has to be provided in the script as longitude and latitude in WGS84 coordinates (degrees) and must be the same as used in program "Preprocessing_Linkdata.R".
2. Read the mean path-averaged link rainfall depths for each time interval.
3. Compute the coordinates belonging to the middle of the links.
4. Determine the unique coordinates of the middle of the links.
5. Calculate the average rainfall depth for each unique set of coordinates. This implies that data from full-duplex links are averaged. If another link happens to have the same middle of the link path, its rainfall depth is taken into account in the averaging.
6. Convert rainfall depths to rainfall intensities ($mm\,h^{-1}$).
7. Compute values of the spherical variogram parameters nugget, sill, and range. These vary with day of year.
8. Apply ordinary kriging to obtain rainfall intensity maps for the provided grid. The 50 nearest observations are used in order to reduce computational time.
9. Negative rainfall values are replaced by zero values.

AMTD
8, 8191–8230, 2015

The spherical variogram parameters are computed as follows (power-law scaling in cosine function parameter; Van de Beek et al., 2012):

$$r = \left(15.51D^{0.09} + 2.06D^{-0.12}\cos\left(\frac{2\pi(\mathrm{DOY} - 7.37D^{0.22})}{365}\right)\right)^4, \quad (12)$$

$$C = \left(0.84D^{-0.25} + 0.20D^{-0.37}\cos\left(\frac{2\pi(\mathrm{DOY} - 162D^{-0.03})}{365}\right)\right)^4, \quad (13)$$

$$C_0 = 0.1C, \quad (14)$$

where r is the range (km), C is the sill (mm^2 h^{-2}), C_0 is the nugget (mm^2 h^{-2}), DOY is day of year, and D is the duration (h). The nugget is basically the variance at zero distance, which can be interpreted as very-fine scale variability or as measurement uncertainty. The sill is the variance at very large distances, and the range is the distance at which the variance does not increase any more (this is equivalent to the distance over which the field is completely decorrelated, i.e., $\rho(r) = 0$). The spherical variogram has the following form:

$$\gamma(h) = \begin{cases} C\left[\frac{3}{2}\frac{h}{r} - \frac{1}{2}\left(\frac{h}{r}\right)^3\right] + C_0 & \text{if} \quad h \le r \\ C + C_0 \quad \text{if} \quad h > r, \end{cases} \quad (15)$$

where h is the distance (m). The program "Interpolation_Rainfall_Intensities.R" only gives the rainfall intensity (mm h^{-1}) as output. Each row corresponds with the same row from the interpolation grid as provided by the file "InterpolationGrid.dat".

AMTD
8, 8191–8230, 2015

Figure 7 shows an example of the interpolation procedure for a given 15 min time interval. The left panel shows the locations of the microwave links, where the colour denotes the rainfall depth. Next, these path-averaged rainfall depths are assigned to the middle of the link, i.e., considered as point measurements (centre panel). This is done to simplify the interpolation procedure. The right panel shows the corresponding interpolated rainfall map.

After it has been explained how the data for rainfall maps can be retrieved from received signal powers of microwave links, the maps are compared to gauge-adjusted radar rainfall maps. The program "RainfallMapping.R" makes a link-based and gauge-adjusted 15 min rainfall map. Moreover, the 15 min rainfall intensities are accumulated to daily rainfall depths, which are visualised. Again the middle of the coordinate system has to be provided and must be the same as used in program "Preprocessing_Linkdata.R". The program has to be modified for application to other time intervals, although some preparations have already been made.

Figures 8 and 9 give an example of 15 min and daily rainfall maps, respectively. The left panels show the link-based rainfall maps, whereas the radar rainfall maps are given in the right panel. The cellular communication network is able to detect the rainfall patterns for the 15 min interval, although deviations are found with respect to radars combined with rain gauges. Note that some large areas do not have link data, as shown in Fig. 7 (left panel). The daily rainfall maps are from 10 September 2011 08:00 UTC–11 September 2011 08:00 UTC and reveal link-based rainfall depths up to 35 mm. In general the link network is able to correctly determine the spatial rainfall patterns. These examples demonstrate a successful application of microwave links to estimate rainfall. Although such a performance has been reported before (Overeem et al., 2013), this is certainly not the case year round. This will be studied in future work.

AMTD
8, 8191–8230, 2015

4 Conclusions

Microwave links from cellular communication networks have been shown to be able to successfully retrieve rainfall information in several studies. For instance, country-wide rainfall maps can be obtained from received signal powers of microwave links (Overeem et al., 2013). In this paper a detailed description is given of a slightly adapted version of the algorithm of Overeem et al. (2013) and of the accompanying code, which is made publicly available with the publication of this paper (see Supplement) under the condition of version 3 of the GNU General Public License. By doing so, we hope to promote the application of rainfall monitoring using microwave links in poorly gauged regions around the world.

Using one processor (Intel i7; Linux operating system) the entire processing takes around 10 min per day, i.e., to obtain the data for 15 min link-based rainfall maps for an entire day based on data from on average 2309 links and 2399 links in total (1484 unique link paths in total). This involves running all programs in Fig. 2 and the program "Figure_Timeseries_Power_Rainfall.R", and hence the production of Figs. 6, 8, and 9. The programs "WetDryClassification_LinkApproach.R" and "Interpolation_Rainfall_Intensities.R" take most processing time, around 4 and 4.5 min, respectively. Slightly more time would be needed in case multiple processors would be used to run multiple days, each processor running its own day. In order to reduce computational time it could be worthwhile to divide a region into sub-regions, particularly to speed up the wet-dry classification.

The rainfall retrieval algorithm is suitable for real-time application. Note that the algorithm is designed for computing rainfall over the previous 24 h and requires the link data from the previous 48 h. If the algorithm would be rerun for another 24 h period, for instance one time interval later, this can result in different rainfall estimates compared to the preceding run. This is due to the wet-dry classification methodology, which may also classify the previous 30 min as rainy. However, in real-time applications the reclassification of previous time intervals is of no consequence. Hence, in order to obtain

AMTD
8, 8191–8230, 2015

the same rainfall estimates for different runs, the algorithm would need to be slightly modified or one should wait 30 min before applying the algorithm in a real-time setting.

The wet-dry classification by means of the link approach leads to a reduction from 2472 to 2428 links. This is caused by a link being selected only if sufficient links are available within a 15 km radius. In case the link approach would reduce the number of links too much, due to a low link density, other wet-dry classification methods should be considered. If available, radar data could be utilised (Overeem et al., 2011). Van het Schip et al. (2015) show that geostationary satellite data hold a promise for wet-dry classification. Such data have a time resolution of 15 min and cover a large part of the globe. Hence, merging of link and satellite data can be a way forward.

Some of the signal fluctuations that occur in dry weather may also occur during rainy periods. The algorithm does not correct for such errors. Furthermore, nearby links may suffer simultaneously from signal fluctuations not caused by rainfall, resulting in a poor performance of the link approach.

Note that the wet antenna attenuation correction A_a will not only compensate for wet antennas. The value of A_a found in the calibration will also be influenced by other errors. Moreover, in case of rain along the link path no, one or both antennas can be wet, whereas this correction is always applied, and A_a itself has also been optimised on data where the number of wet antennas can vary. In addition, the correction does not depend on rainfall intensity. Hence, applying A_a should be seen as an attempt to correct for wet antennas. Further, the coefficient α is employed to obtain mean path-averaged rainfall intensities from minimum and maximum path-averaged rainfall intensities. It is advised to recalibrate A_a and α in case of other networks or climates. This may be achieved by comparing link-based rainfall estimates with high-quality (gauge-adjusted) weather radar data, which may provide full coverage over the network, as in Overeem et al. (2013). Alternatively, path-averaged rainfall intensities may be estimated from rain gauge data. This may require a dedicated research experiment (Minda and Nakamura, 2005; Wang et al., 2012), preferably with several rain gauges along the link path. Such an experiment has started in Wageningen, the Netherlands, including, among others,

AMTD
8, 8191–8230, 2015

a former commercial microwave link. If neither ground-based radars nor rain gauges are available, satellite-based precipitation products could be employed. For instance, the new IMERG product of the Global Precipitation Measurement mission (GPM) is a gridded rainfall data set covering 60° N–60° S with a spatial resolution of 0.1° and a temporal resolution of 30 min (Hou et al., 2014). This is particularly interesting for countries with few surface rainfall observations. Note that large revisit times and the relatively coarse spatial resolution with respect to the path lengths pose a constraint. The former does not entirely hold for geostationary satellites with a time resolution of typically 15 min, but then rainfall estimation is rather indirect from, e.g., cloud physical properties (Roebeling and Holleman, 2009). Finally, see, for instance, Leijnse et al. (2007b, 2008); Schleiss et al. (2013) for another wet antenna attenuation correction method.

The derivation of mean path-averaged rainfall intensities from minimum and maximum rainfall intensities is simple and may be improved by performing an experiment. The value of α is expected to depend on the time variability of rainfall. Messer et al. (2006) use the known distribution of rainfall intensities at the point scale to weigh minimum and maximum received signal levels. If a (former) commercial microwave link could be sampled at high frequency, e.g., 10 Hz, minimum, maximum, but also mean received signal power could be derived for time intervals of a given length. Overeem et al. (2011) utilise a research link with high temporal resolution for testing the proposed rainfall retrieval algorithm. By applying the rainfall retrieval algorithm mean path-averaged rainfall intensities can be derived. These can be compared to the corresponding values obtained from the mean received signal power. Hence, the same instrument, a microwave link, is used to assess the ability of the retrieval algorithm to deal with the sampling strategy. Since the same instrument is used representativeness errors are not present. The probability distribution of minimum and maximum rainfall intensities could be studied in order to obtain more reliable mean rainfall intensities. Moreover, such an experiment may also help to assess attenuation due to wet antennas caused by dew or rain, its dependence on rainfall intensity or antenna cover type, and the time

AMTD
8, 8191–8230, 2015

it takes for antennas to become dry. Preferably a rain gauge or disdrometer is available near the antenna.

The value of the exponent b is close to 1 for the frequencies employed in this study, which range from 13–40 GHz. Frequencies between 37 and 40 GHz are denoted by the gray-shaded area in Fig. 5, which contains 81 % of the links from the working example, even having a value of b very close to 1 (right). For other frequencies the corresponding value of b often deviates more from 1 (Fig. 5, right). High rainfall variability along the link path will lead to overestimation for $b < 1$ and underestimation for $b > 1$. In the tropics also lower frequencies, such as 7 GHz, are used, which will lead to overestimation.

The code can be applied to other link networks with the same sampling strategy, i.e., minimum and maximum received powers per 15 min interval. The entire code can also be adapted to other sampling strategies. In case of minimum and maximum received powers over other time intervals this can be easily changed in the top of the scripts up to and including "Interpolation_Rainfall_Intensities.R". The number of time intervals per 24 h period should be an integer. Although the code should work for other time intervals, such as 5 min, it is recommended to test the code first in such a case. Note that coefficients and thresholds have been optimised for 15 min intervals and that their values may not be appropriate for other time intervals. In case of very different sampling strategies, e.g., mean or instantaneous received signal powers for shorter or longer time intervals, the code should be modified. For instance, the link approach to detect wet and dry periods should also work, but is expected to require, at least, other threshold values. In general it could be important to find optimal threshold values for other climates or networks, even if the same sampling strategy as for the network in this paper would be employed.

Other networks may not operate with constant transmitted powers, i.e., the transmit power can become higher in case of a reduced received power at the end of the link. These links use Automatic Transmit Power Control (ATPC). In this case the transmitted power also needs to be known and should be taken into account in the rainfall retrieval algorithm (Schleiss and Berne, 2010; Doumounia et al., 2014). Note that a sampling

AMTD
8, 8191–8230, 2015

strategy where minimum and maximum transmitted and received powers are available over a chosen time interval may result in additional errors. The timing of minimum received and transmitted powers does not necessarily coincide, which also holds for the maximum powers.

Table 2 gives an overview of the parameters of the rainfall retrieval algorithm, their values and the factors influencing them. This can help to assess which parameters will change for other regions and networks.

The employed interpolation methodology, ordinary kriging, may not be specifically suited for other regions with different rainfall climatologies. The methodology developed in Van de Beek et al. (2012) could be optimised for other climates. This requires long rainfall time series. The assumed stationarity and isotropy will often be violated (Schuurmans et al., 2007). Moreover, the path-averaged link rainfall intensities are assumed to be point measurements. Hence, it is recommended to improve the interpolation methodology, e.g., by treating the rainfall values as path instead of as point observations, which is expected to have the largest impact for areas with high link densities or with long links. Using data from the same 12 days as used in Overeem et al. (2013); Rios Gaona et al. (2015) find that link rainfall retrieval errors themselves are the source of error that contributes most to the overall uncertainty in rainfall maps from a commercial link network. Errors due to interpolation methodology play a minor, but non-negligible role in case of country-wide rainfall maps obtained for the network and climate of the Netherlands.

In this paper data from one network have been utilised. In case data from more networks, either from the same or from different providers, are available, these can simply be combined into one file per day. The only requirements are that unique link identifiers are employed and that these networks use the same sampling strategy.

The Supplement related to this article is available online at doi:10.5194/amtd-8-8191-2015-supplement.

AMTD
8, 8191–8230, 2015

Acknowledgements. We gratefully acknowledge Ronald Kloeg and Ralph Koppelaar from T-Mobile NL for providing the cellular communication link data. We thank Marc Bierkens (Utrecht University) for his advice concerning kriging and Manuel Rios Gaona for programming part of the kriging script. This work was financially supported by the Netherlands Technology Foundation STW (project 11944).

References

Atlas, D. and Ulbrich, C. W.: Path- and area-integrated rainfall measurement by microwave attenuation in the 1–3 cm band, J. Appl. Meteorol., 16, 1322–1331, 1977. 8203

Berne, A. and Uijlenhoet, R.: Path-averaged rainfall estimation using microwave links: uncertainty due to spatial rainfall variability, Geophys. Res. Lett., 34, L07403, doi:10.1029/2007GL029409, 2007. 8204

Bianchi, B., Rieckermann, J., and Berne, A.: Quality control of rain gauge measurements using telecommunication microwave links, J. Hydrol., 492, 15–23, doi:10.1016/j.jhydrol.2013.03.042, 2013. 8193, 8195

Chwala, C., Gmeiner, A., Qiu, W., Hipp, S., Nienaber, D., Siart, U., Eibert, T., Pohl, M., Seltmann, J., Fritz, J., and Kunstmann, H.: Precipitation observation using microwave backhaul links in the alpine and pre-alpine region of Southern Germany, Hydrol. Earth Syst. Sci., 16, 2647–2661, doi:10.5194/hess-16-2647-2012, 2012. 8192, 8195, 8198

Doumounia, A., Gosset, M., Cazenave, F., Kacou, M., and Zougmore, F.: Rainfall monitoring based on microwave links from cellular telecommunication networks: first results from a West African test bed, Geophys. Res. Lett., 41, 6016–6022, doi:10.1002/2014GL060724, 2014. 8193, 8198, 8214

Heistermann, M., Jacobi, S., and Pfaff, T.: Technical Note: An open source library for processing weather radar data (*wradlib*), Hydrol. Earth Syst. Sci., 17, 863–871, doi:10.5194/hess-17-863-2013, 2013. 8192

Hou, A. Y., Kakar, R. K., Neeck, S., Azarbarzin, A. A., Kummerow, C. C., Kojima, M., Oki, R., Nakamura, K., and Iguchi, T.: The global precipitation measurement mission, B. Am. Meteorol. Soc., 95, 701–722, doi:10.1175/BAMS-D-13-00164.1, 2014. 8213

Kharadly, M. M. Z. and Ross, R.: Effect of wet antenna attenuation on propagation data statistics, IEEE T. Antenn. Propag., 49, 1183–1191, 2001. 8205

AMTD
8, 8191–8230, 2015

Leijnse, H., Uijlenhoet, R., and Stricker, J. N. M.: Rainfall measurement using radio links from cellular communication networks, Water Resour. Res., 43, W03201, doi:10.1029/2006WR005631, 2007a. 8192, 8195, 8198, 8205

Leijnse, H., Uijlenhoet, R., and Stricker, J. N. M.: Hydrometeorological application of a microwave link: 2. Precipitation, Water Resour. Res., 43, W04417, doi:10.1029/2006WR004989, 2007b. 8205, 8213

Leijnse, H., Uijlenhoet, R., and Stricker, J. N. M.: Microwave link rainfall estimation: effects of link length and frequency, temporal sampling, power resolution, and wet antenna attenuation, Adv. Water Resour., 31, 1481–1493, doi:10.1016/j.advwatres.2008.03.004, 2008. 8203, 8204, 8205, 8213, 8221

Leijnse, H., Uijlenhoet, R., and Berne, A.: Errors and uncertainties in microwave link rainfall estimation explored using drop size measurements and high-resolution radar data, J. Hydrometeorol., 11, 1330–1344, doi:10.1175/2010JHM1243.1, 2010. 8204

Lorenz, C. and Kunstmann, H.: The hydrological cycle in three state-of-the-art reanalyses: intercomparison and performance analysis, J. Hydrometeorol., 13, 1397–1420, doi:10.1175/JHM-D-11-088.1, 2012. 8192

Messer, H. A., Zinevich, A., and Alpert, P.: Environmental monitoring by wireless communication networks, Science, 312, p. 713, 2006. 8192, 8195, 8198, 8213

Minda, H. and Nakamura, K.: High temporal resolution path-average rain gauge with 50-GHz band microwave, J. Atmos. Ocean. Tech., 22, 165–179, 2005. 8205, 8212

Olsen, R. L., Rogers, D. V., and Hodge, D. B.: The aR^b relation in the calculation of rain attenuation, IEEE T. Antenn. Propag., 26, 318–329, 1978. 8203

Overeem, A., Buishand, T. A., and Holleman, I.: Extreme rainfall analysis and estimation of depth-duration-frequency curves using weather radar, Water Resour. Res., 45, W10424, doi:10.1029/2009WR007869, 2009a. 8196

Overeem, A., Holleman, I., and Buishand, T. A.: Derivation of a 10-year radar-based climatology of rainfall, J. Appl. Meteorol. Clim., 48, 1448, doi:10.1175/2009JAMC1954.1, 2009b. 8196

Overeem, A., Leijnse, H., and Uijlenhoet, R.: Measuring urban rainfall using microwave links from commercial cellular communication networks, Water Resour. Res., 47, W12505, doi:10.1029/2010WR010350, 2011. 8192, 8193, 8196, 8198, 8199, 8200, 8204, 8206, 8212, 8213

AMTD
8, 8191–8230, 2015

Overeem, A., Leijnse, H., and Uijlenhoet, R.: Country-wide rainfall maps from cellular communication networks, P. Natl. Acad. Sci. USA, 110, 2741–2745, doi:10.1073/pnas.1217961110, 2013. 8192, 8193, 8196, 8198, 8200, 8202, 8206, 8210, 8211, 8212, 8215

Rayitsfeld, A., Samuels, R., and Zinevich, A.: Comparison of two methodologies for long term rainfall monitoring using a commercial microwave communication system, Atmos. Res., 104–105, 119–127, doi:10.1016/j.atmosres.2011.08.011, 2012. 8192, 8195, 8198

Rios Gaona, M. F., Overeem, A., Leijnse, H., and Uijlenhoet, R.: Sources of uncertainty in rainfall maps from cellular communication networks, Hydrol. Earth Syst. Sci. Discuss., 12, 3289–3317, doi:10.5194/hessd-12-3289-2015, 2015. 8194, 8215

Roebeling, R. A. and Holleman, I.: SEVIRI rainfall retrieval and validation using weather radar observations, J. Geophys. Res., 114, D21202, doi:10.1029/2009JD012102, 2009. 8213

Schleiss, M. and Berne, A.: Identification of dry and rainy periods using telecommunication microwave links, IEEE Geosci. Remote S., 7, 611–615, doi:10.1109/LGRS.2010.2043052, 2010. 8198, 8214

Schleiss, M., Rieckermann, J., and Berne, A.: Quantification and modeling of wet-antenna attenuation for commercial microwave links, IEEE Geosci. Remote S., 10, 1195–1199, doi:10.1109/LGRS.2012.2236074, 2013. 8213

Schuurmans, J. M., Bierkens, M. F. P., Pebesma, E. J., and Uijlenhoet, R.: Automatic prediction of high-resolution daily rainfall fields for multiple extents: the potential of operational radar, J. Hydrometeorol., 8, 1204–1224, doi:10.1175/2007JHM792.1, 2007. 8215

Upton, G. J. G., Holt, A. R., Cummings, R. J., Rahimi, A. R., and Goddard, J. W. F.: Microwave links: the future for urban rainfall measurement?, Atmos. Res., 77, 300–312, doi:10.1016/j.atmosres.2004.10.009, 2005. 8198

Van de Beek, C. Z., Leijnse, H., Torfs, P. J. J. F., and Uijlenhoet, R.: Seasonal semi-variance of Dutch rainfall at hourly to daily scales, Adv. Water Resour., 45, 76–85, doi:10.1016/j.advwatres.2012.03.023, 2012. 8207, 8209, 8215

Van het Schip, T. I., Overeem, A., Leijnse, H., Uijlenhoet, R., Meirink, J. F., and van Delden, A. J.: Rainfall measurement using cell phone links: classification of wet and dry periods using satellites, Meteorol. Appl., in prep., 2015. 8198, 8212

Wang, Z., Schleiss, M., Jaffrain, J., Berne, A., and Rieckermann, J.: Using Markov switching models to infer dry and rainy periods from telecommunication microwave link signals, Atmos. Meas. Tech., 5, 1847–1859, doi:10.5194/amt-5-1847-2012, 2012. 8198, 8212

AMTD
8, 8191–8230, 2015

Zinevich, A., Messer, H., and Alpert, P.: Frontal rainfall observation by a commercial microwave communication network, J. Appl. Meteorol. Clim., 48, 1317, doi:10.1175/2008JAMC2014.1, 2009. 8192

AMTD
8, 8191–8230, 2015

Table 1. Variables used in the programs of the rainfall retrieval algorithm. The numbered programs can be found in Fig. 2.

Header name	Symbol in text	Unit	Description	Appears in program(s)
a	a	mm h^{-1} dB^{-b} km^{b}	Coefficient of R–k power law	2, 3
Am_max	A_{max}	dB	Maximum rain-induced attenuation	2, 3
Am_min	A_{min}	dB	Minimum rain-induced attenuation	2, 3
b	b	–	Exponent of R–k power law	2, 3
DATETIME	N/A	UTC	Date and time	1, 2
F	F	km^{-1} h	Filter to remove outliers	2, 3
Frequency	f	GHz	Microwave frequency	1, 2, 3
ID	ID	–	Unique link identifier	1, 2, 3, 4
interval_number	N/A	–	Time interval number	1, 2, 3, 4
meanval	N/A	–	Average number of surrounding links in wet-dry classification	2
path_length	L	km	Path length	1, 2, 3
rainfall_depth_path	N/A	mm	Path-averaged rainfall depth	3, 4
rain_intensity	$\langle R \rangle$	mm h^{-1}	Path-averaged rainfall intensity	4, 5
ref_level	P_{ref}	dB	Reference level	2
RXMIN	P_{min}	dB	Minimum received power	1, 2
RXMIN_final	P^{C}_{min}	dB	Corrected minimum received power	2
RXMAX	P_{max}	dB	Maximum received power	1, 2
RXMAX_final	P^{C}_{max}	dB	Corrected maximum received power	2
x_start	N/A	° (km)	Longitude (or easting) of start of microwave link	1 (1, 2, 3)
x_end	N/A	° (km)	Longitude (or easting) of end of microwave link	1 (1, 2, 3)
y_start	N/A	° (km)	Latitude (or northing) of start of microwave link	1 (1, 2, 3)
y_end	N/A	° (km)	Latitude (or northing) of end of microwave link	1 (1, 2, 3)

AMTD
8, 8191–8230, 2015

Table 2. Values of the parameters used in the rainfall retrieval algorithm.

Variable description	Symbol and unit	Value	Depends on:
Threshold wet-dry classification	median(ΔP_L)	$-0.7\,\mathrm{dB\,km^{-1}}$	Spatial correlation of rainfall
Threshold wet-dry classification	median(ΔP)	−1.4 dB	Spatial correlation of rainfall
Radius in wet-dry classification	r	15 km	Spatial correlation of rainfall
Filter to remove outliers	F	$-32.5\,\mathrm{dB\,km^{-1}\,h}$	Malfunctioning of links
Wet antenna attenuation	A_a (dB)	2.3	Rainfall intensity, number of wet antennas, antenna cover[1]
Coefficient	α (–)	0.33	Time variability of rainfall[2]
Coefficient of R–k power law	a ($\mathrm{mm\,h^{-1}\,dB^{-b}\,km^{b}}$)	3.4–25.0	Drop size distribution, frequency[3]
Exponent of R–k power law	b (–)	0.81–1.06	Drop size distribution, frequency[3]

[1] Here A_a is fixed.
[2] Here α is fixed.
[3] And to some extent on polarization, temperature, drop shape, and canting angle distribution (this has not been taken into account). Here values have been computed from one data set of measured drop size distributions (Leijnse et al., 2008).

AMTD
8, 8191–8230, 2015

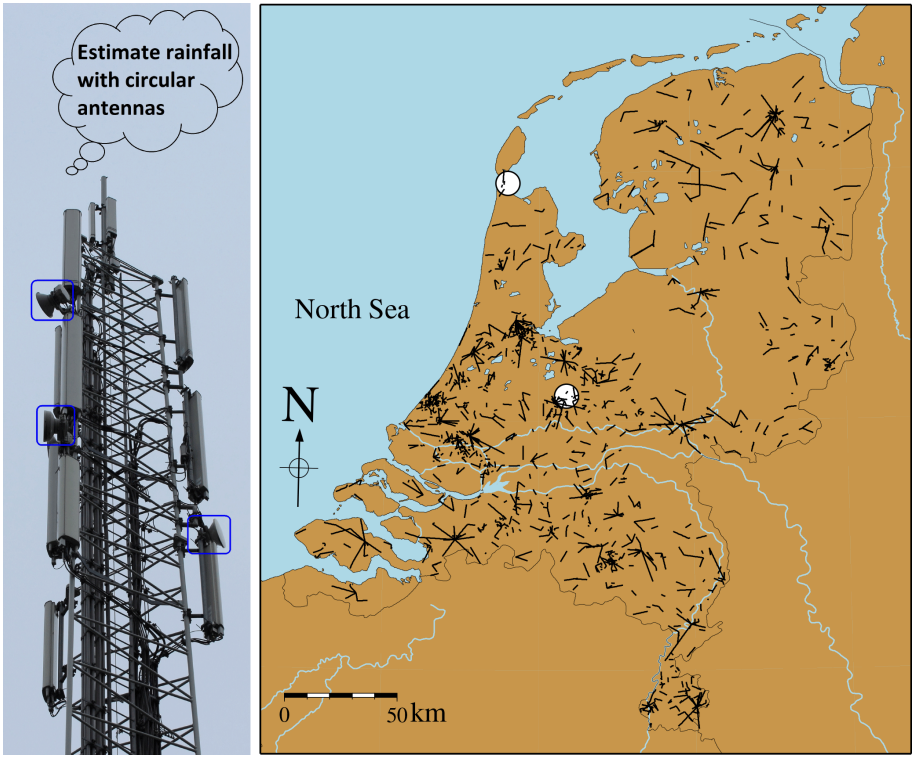

Figure 1. Left: illustration of a telephone tower. The electromagnetic signals transmitted from the circular antenna of one cellular communication tower to another are attenuated by rainfall. Right: map of the Netherlands with locations of the employed link paths (1484) from the cellular communication network for 10 September, 08:00 UTC–11 September, 08:00 UTC (2011). These were part of one network of one of the three providers in the Netherlands. The white circles show the locations of the radars.

AMTD
8, 8191–8230, 2015

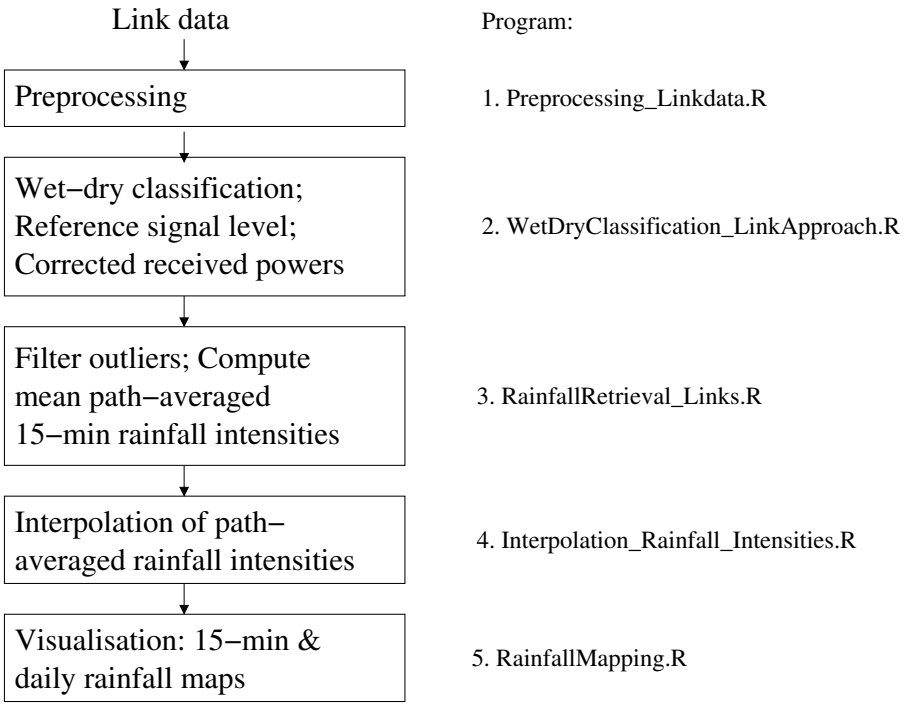

Figure 2. Flowchart of processing link data. From received signal powers to rainfall maps.

AMTD
8, 8191–8230, 2015

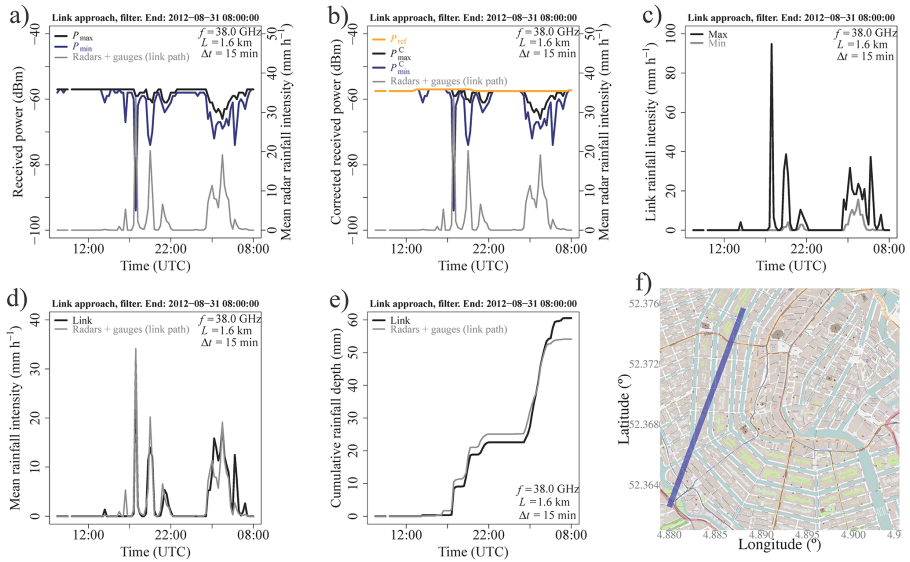

Figure 3. From received signal powers to cumulative rainfall depths (one day, one link). Minimum and maximum received powers and path-averaged, gauge-adjusted radar rainfall intensities **(a)**. Corrected minimum and maximum received powers and path-averaged, gauge-adjusted radar rainfall intensities **(b)**. Minimum and maximum path-averaged link rainfall intensities **(c)**. Mean path-averaged link and gauge-adjusted rainfall intensities **(d)**. Cumulative path-averaged link and gauge-adjusted radar rainfall depths **(e)**. Map with location of microwave link in Amsterdam City, the Netherlands **(f)**. Period: 30 August, 08:00 UTC–31 August, 08:00 UTC (2012).

AMTD
8, 8191–8230, 2015

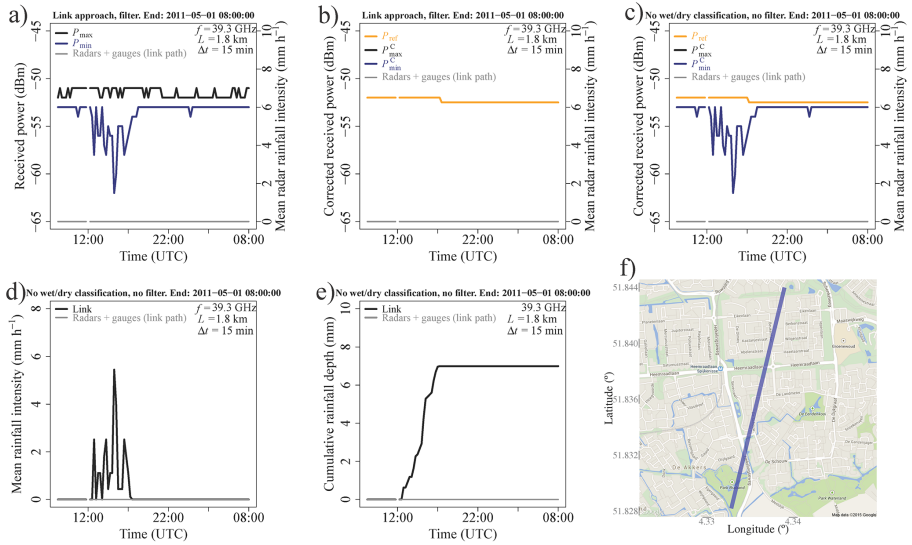

Figure 4. Time series for which the link approach works well and is necessary (one day, one link). The link-based rainfall information has been computed without applying a wet-dry classification. This results in a large overestimation. See Fig. 3 for description of the time series. Map with location of microwave link in Spijkenisse, the Netherlands. Period: 30 April, 08:00 UTC–1 May, 08:00 UTC (2011; **f**).

AMTD
8, 8191–8230, 2015

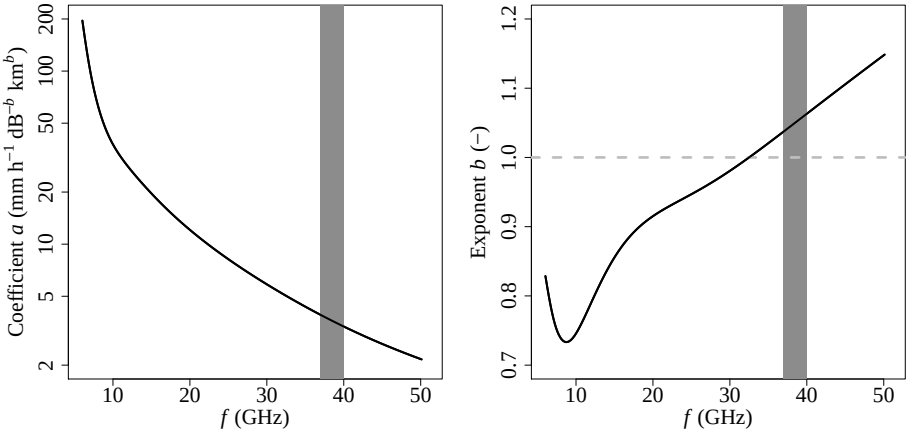

Figure 5. Values of coefficients in the R–k relation for vertically polarised signals for frequencies ranging from 6 to 50 GHz. The gray-shaded area denotes the 37–40 GHz range. Note the logarithmic vertical scale in the left figure.

AMTD
8, 8191–8230, 2015

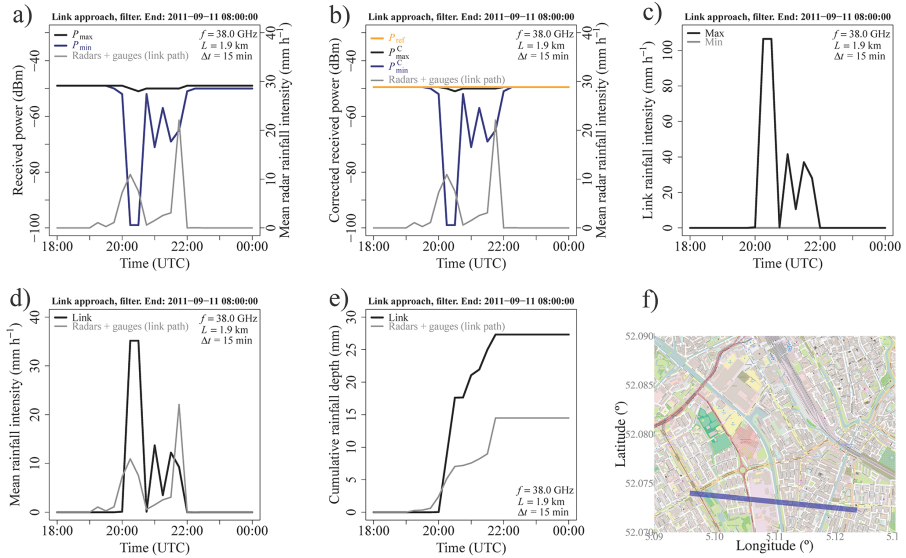

Figure 6. Illustration of the rainfall retrieval algorithm (one link). See Fig. 3 for description of the time series. Map with location of microwave link in Utrecht, the Netherlands. Period: 10 September 18:00–24:00 UTC (2011; **f**). This figure is part of the working example.

AMTD
8, 8191–8230, 2015

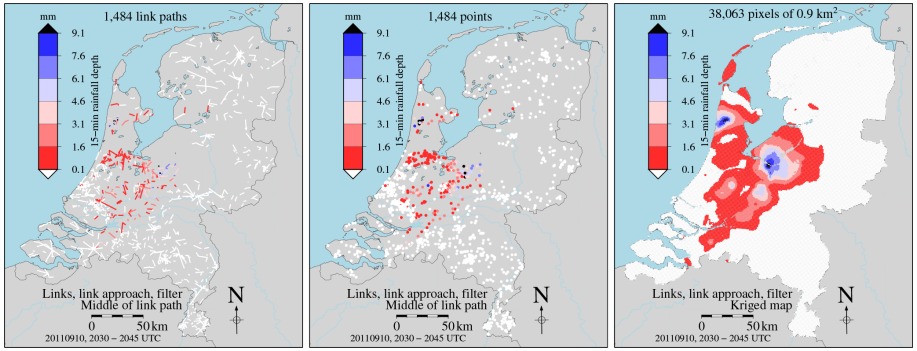

Figure 7. From path-averaged link rainfall depths to link rainfall maps. Assign path observations (left) to points (centre). Apply ordinary kriging to obtain rainfall maps (right). For time interval 20:30–20:45 UTC on 10 September 2011.

AMTD
8, 8191–8230, 2015

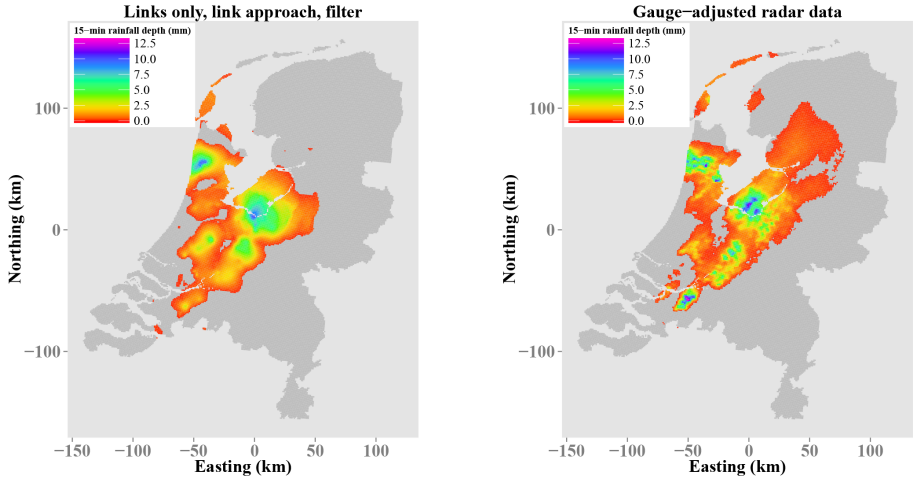

Figure 8. 15 min rainfall maps from 10 September 20:30–20:45 UTC (2011), for links only and radars plus gauges for the Netherlands. Spatial resolution: approximately 0.9 km^2. Values below 0.1 mm are not shown. This figure is part of the working example.

AMTD
8, 8191–8230, 2015

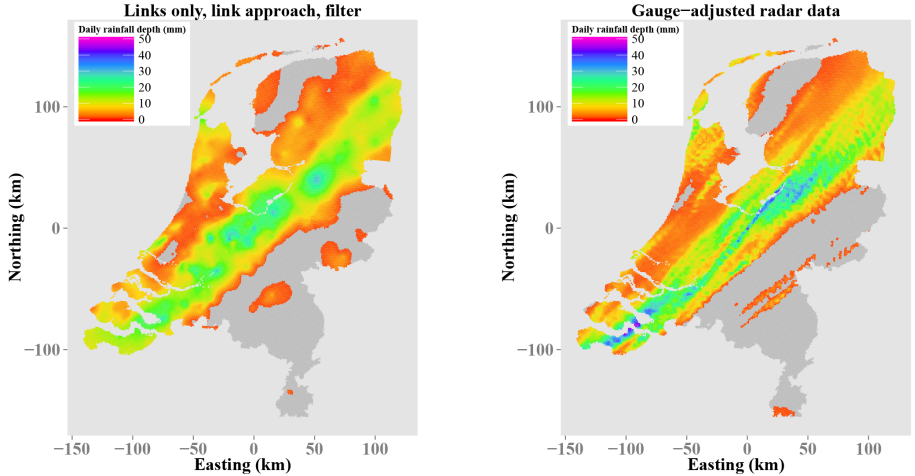

Figure 9. Daily rainfall maps for links only and radars plus gauges for the Netherlands. Spatial resolution: approximately 0.9 km^2. Period: 10 September, 08:00 UTC–11 September, 08:00 UTC (2011). Values below 1 mm are not shown. This figure is part of the working example.

AMTD
8, 8191–8230, 2015